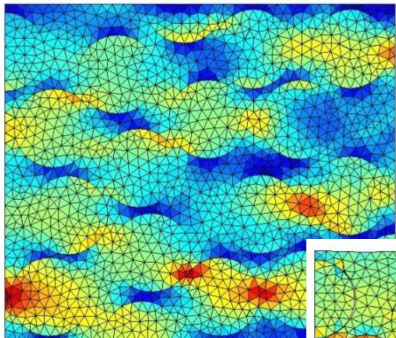

A micro-model of the intra-laminar fracture in fiber-reinforced composites based on a discontinuous Galerkin/extrinsic cohesive law method

L. Wu (ULg), D. Tjahjanto (KTH), G. Becker (MIT),
A. Makradi (CRPHT), A. Jérusalem (Oxford),
L. Noels (ULg)
,

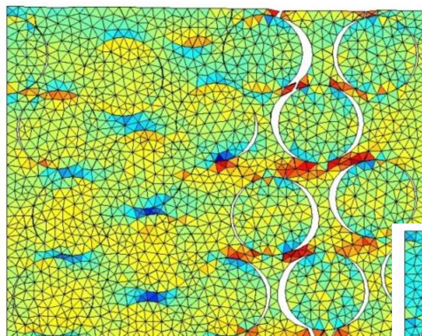

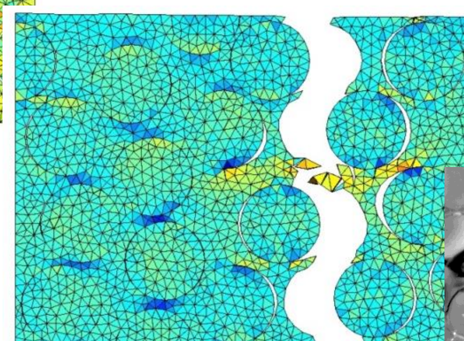

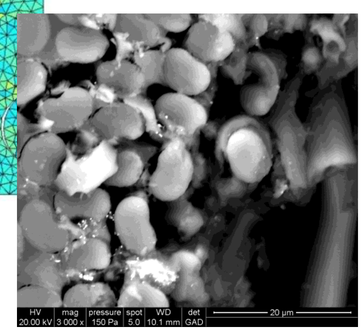

SIMUCOMP The research has been funded by the Walloon Region under the agreement no 1017232 (CT-EUC 2010-10-12) in the context of the ERA-NET +, Matera + framework.

Content

- Introduction
  - Fracture modelling
- Hybrid discontinuous-Galerkin/ Extrinsic cohesive law framework
  - DG methods
  - Hybrid method
  - Parallel implementation
- Application to intra-laminar failure of composites
  - Numerical simulations
  - Micro-Meso fracture model
- Conclusions

- Intra-laminar fracture challenges
  - Fracture can be
    - At fiber interfaces (debonding)
    - In matrix
  - Initially there is no crack
  - Cell size effect

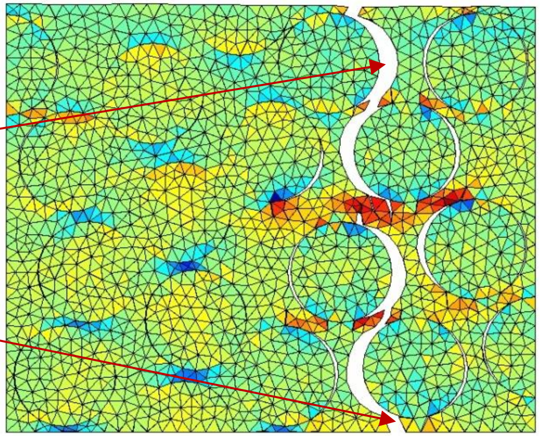

Introduction

- Intra-laminar fracture challenges
  - Fracture can be
    - At fiber interfaces (debonding)
    - In matrix
  - Initially there is no crack
  - Cell size effect

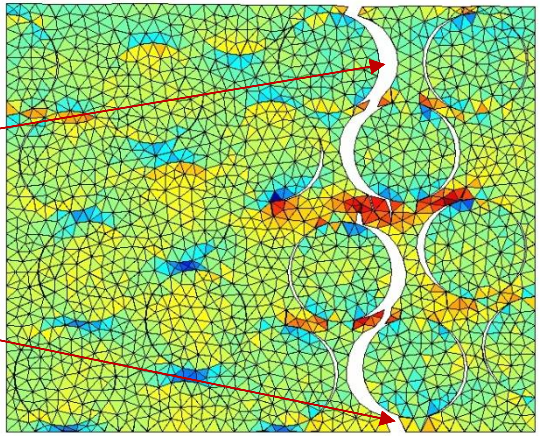

- Numerical approach
  - Cohesive elements inserted between two bulk elements
  - They integrate the cohesive Traction Separation Laws
  - Characterized by
    - Strength σ_c &
    - Critical energy release rate G_C
  - Can be tailored for
    - Debonding
    - Matrix crack

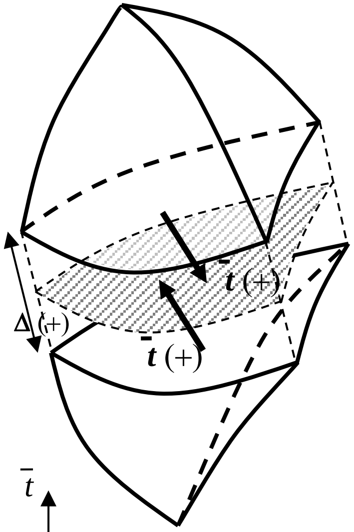

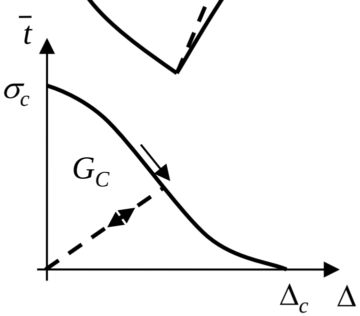

- Problems with cohesive elements
  - Intrinsic Cohesive Law (ICL)
    - Cohesive elements inserted from the beginning
    - Drawbacks:
      - Efficient if a priori knowledge of the crack path
      - Mesh dependency [Xu & Needelman, 1994]
      - Initial slope modifies the effective elastic modulus
      - This slope should tend to infinity [Klein et al. 2001]:
        - Alteration of a wave propagation
        - Critical time step is reduced

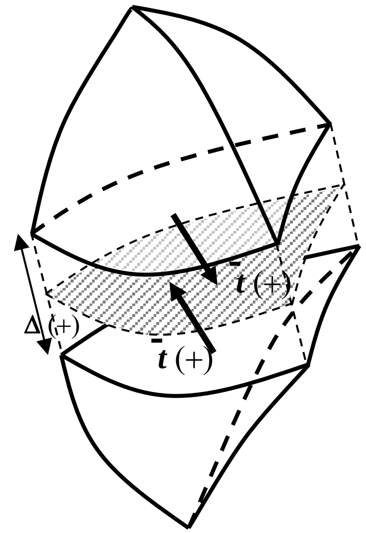

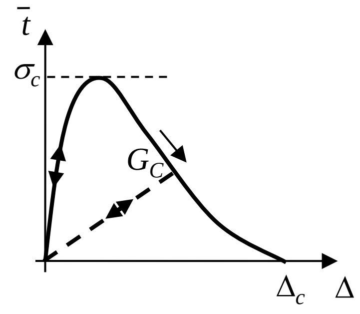

Introduction

- Problems with cohesive elements
  - Intrinsic Cohesive Law (ICL)
    - Cohesive elements inserted from the beginning
    - Drawbacks:
      - Efficient if a priori knowledge of the crack path
      - Mesh dependency [Xu & Needelman, 1994]
      - Initial slope modifies the effective elastic modulus
      - This slope should tend to infinity [Klein et al. 2001]:
        - Alteration of a wave propagation
        - Critical time step is reduced
  - Extrinsic Cohesive Law (ECL)
    - Cohesive elements inserted on the fly when the failure criterion is verified [Ortiz & Pandolfi 1999]
    - Drawback
      - Complex implementation in 3D (parallelization)

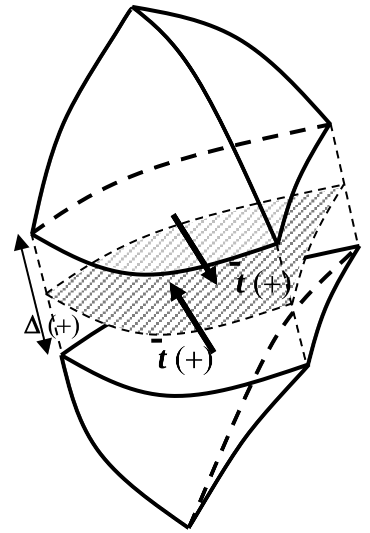

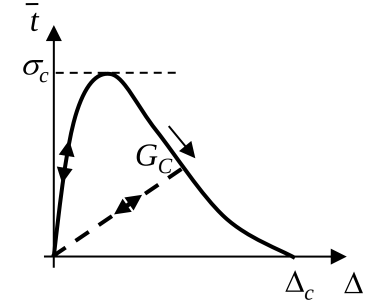

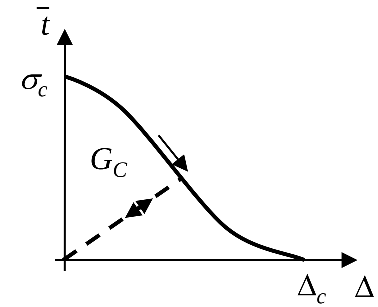

Introduction

- Solution: Discontinuous Galerkin/Extrinsic Cohesive Law method
  - Embeds interface elements
  - Consistent
  - Highly scalable
- Successful applications

Ceramic fragmentation

[Radovitzky et al., CMAME 2011]

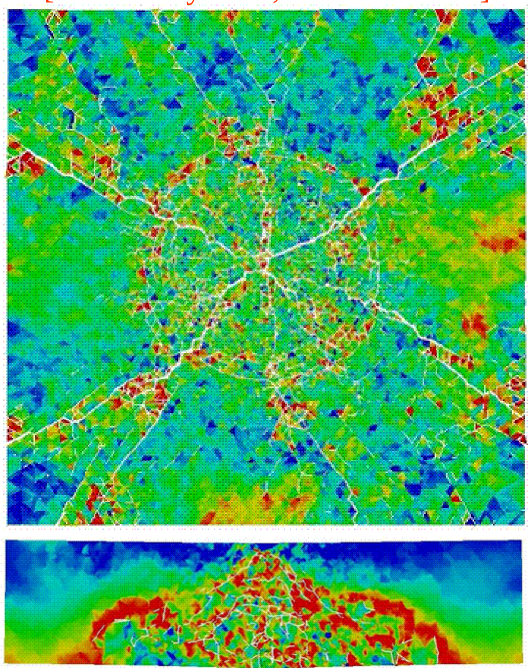

Failure of blast loaded elasto-plastic thin structures

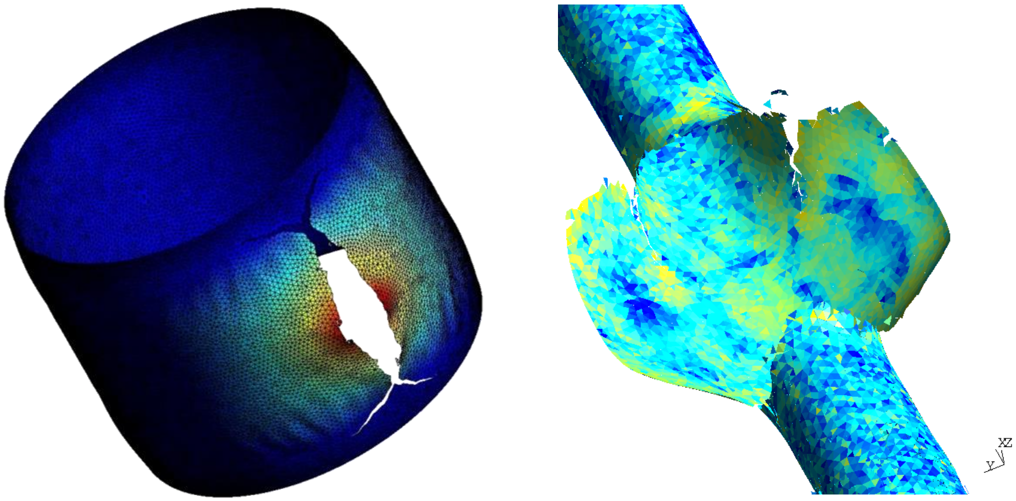

[Becker & Noels., IJNME 2012]

- Discontinuous Galerkin (DG) methods
  - Finite-element discretization
  - Same **discontinuous** polynomial approximations for the
    - **Test** functions φ_h and
    - **Trial** functions $\delta\varphi$

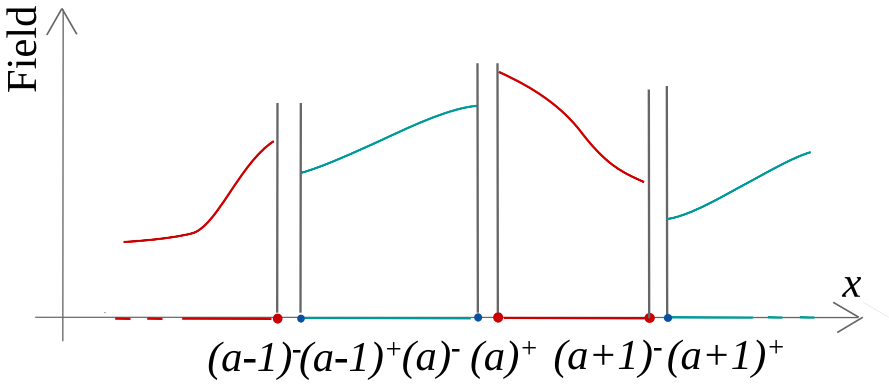

  - Definition of operators on the interface trace:
    - **Jump** operator: $[\![\cdot]\!] = \cdot^+ - \cdot^-$
    - **Mean** operator: $\langle\cdot\rangle = \frac{\cdot^+ + \cdot^-}{2}$
  - Continuity is weakly enforced, such that the method
    - Is consistent
    - Is stable
    - Has the optimal convergence rate

Université de Liège

- Discontinuous Galerkin (DG) methods (2)
  - Formulation in terms of the first Piola-Kirchhoff stress tensor $\mathbf{P}$

$$\boldsymbol{\nabla}_0 \cdot \mathbf{P}^T = 0 \text{ in } \Omega_0 \quad \& \quad \begin{cases} \mathbf{P} \cdot \boldsymbol{N} = \overline{\boldsymbol{T}} \text{ on } \partial_N \Omega_0 \\ \boldsymbol{\varphi} = \overline{\boldsymbol{\varphi}} \text{ on } \partial_D \Omega_0 \end{cases}$$

  - Weak formulation obtained by integration by parts **on each element** Ω^e

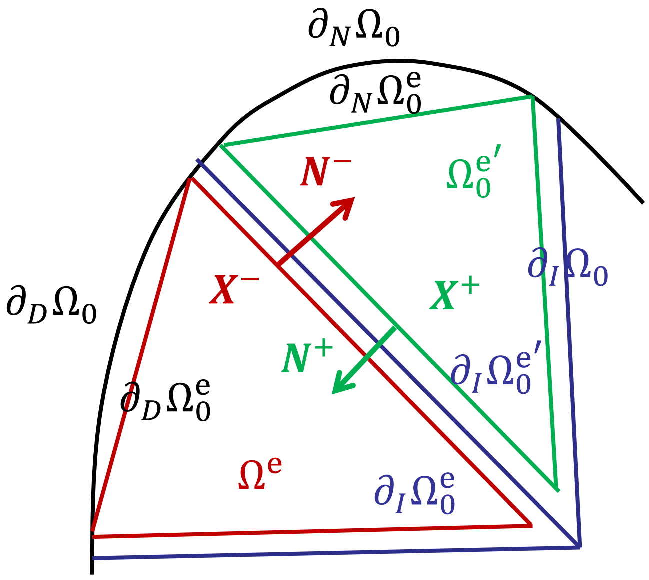

$$\sum_e \int_{\Omega_0^e} \boldsymbol{\nabla}_0 \cdot \mathbf{P}^T \cdot \boldsymbol{\delta\varphi} \, d\Omega = 0$$

- Discontinuous Galerkin (DG) methods (2)
  - Formulation in terms of the first Piola-Kirchhoff stress tensor $\mathbf{P}$

$$\boldsymbol{\nabla}_0 \cdot \mathbf{P}^T = 0 \text{ in } \Omega_0 \quad \& \quad \begin{cases} \mathbf{P} \cdot \boldsymbol{N} = \overline{\boldsymbol{T}} \text{ on } \partial_N \Omega_0 \\ \boldsymbol{\varphi} = \overline{\boldsymbol{\varphi}} \text{ on } \partial_D \Omega_0 \end{cases}$$

  - Weak formulation obtained by integration by parts **on each element** Ω^e

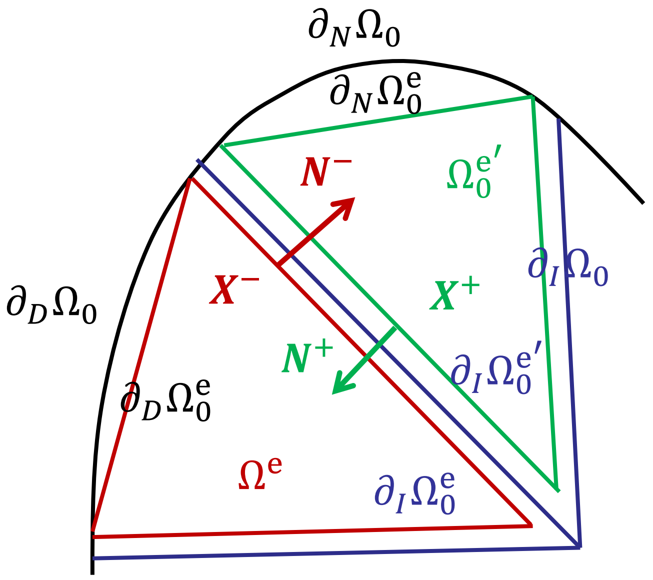

$$\sum_e \int_{\Omega_0^e} \boldsymbol{\nabla}_0 \cdot \mathbf{P}^T \cdot \boldsymbol{\delta\varphi} d\Omega = 0$$

$$\sum_e \int_{\Omega_0^e} -\mathbf{P} : \boldsymbol{\nabla}_0 \boldsymbol{\delta\varphi} d\Omega + \sum_e \int_{\partial\Omega_0^e} \boldsymbol{\delta\varphi} \cdot \mathbf{P} \cdot \boldsymbol{N} d\partial\Omega = 0$$

- Discontinuous Galerkin (DG) methods (2)
  - Formulation in terms of the first Piola-Kirchhoff stress tensor $\mathbf{P}$

$$\nabla_0 \cdot \mathbf{P}^T = 0 \text{ in } \Omega_0 \quad \& \quad \begin{cases} \mathbf{P} \cdot \boldsymbol{N} = \bar{\boldsymbol{T}} \text{ on } \partial_N \Omega_0 \\ \boldsymbol{\varphi} = \bar{\boldsymbol{\varphi}} \text{ on } \partial_D \Omega_0 \end{cases}$$

  - Weak formulation obtained by integration by parts **on each element** Ω^e

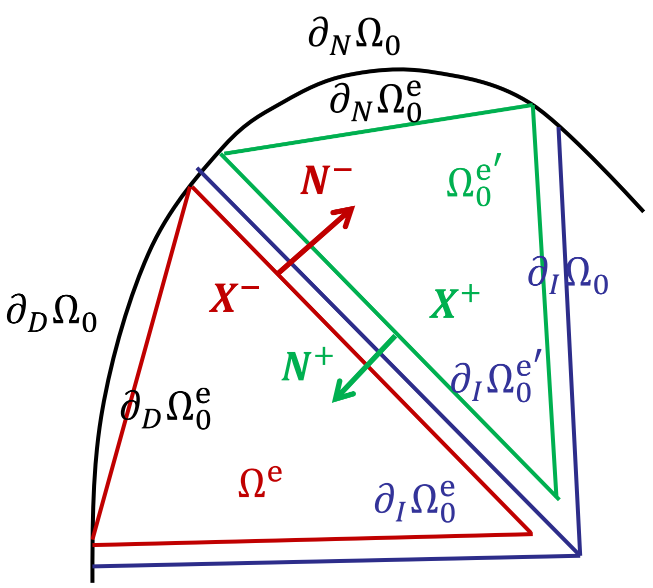

$$\sum_e \int_{\Omega_0^e} \nabla_0 \cdot \mathbf{P}^T \cdot \boldsymbol{\delta\varphi} \, d\Omega = 0$$

$$\sum_e \int_{\Omega_0^e} -\mathbf{P} : \nabla_0 \boldsymbol{\delta\varphi} \, d\Omega + \sum_e \int_{\partial\Omega_0^e} \boldsymbol{\delta\varphi} \cdot \mathbf{P} \cdot \boldsymbol{N} \, d\partial\Omega = 0$$

$$\int_{\Omega_0} \mathbf{P} : \nabla_0 \boldsymbol{\delta\varphi} \, d\Omega + \int_{\partial_I \Omega_0} [\![\boldsymbol{\delta\varphi} \cdot \mathbf{P}]\!] \cdot \boldsymbol{N}^- \, d\partial\Omega = \int_{\partial_N \Omega_0} \bar{\boldsymbol{T}} \cdot \boldsymbol{\delta\varphi} \, d\partial\Omega$$

New interface terms

- Discontinuous Galerkin (DG) methods (3)

$$\int_{\Omega_0} \mathbf{P} : \boldsymbol{\nabla}_0 \boldsymbol{\delta\varphi} d\Omega \ + \int_{\partial_{\mathrm{I}}\Omega_0} [\![\boldsymbol{\delta\varphi} \cdot \mathbf{P}]\!] \cdot \boldsymbol{N}^{-} d\partial\Omega = \int_{\partial_N \Omega_0} \overline{\boldsymbol{T}} \cdot \boldsymbol{\delta\varphi} d\partial\Omega$$

- Discontinuous Galerkin (DG) methods (3)

$$\int_{\Omega_0} \mathbf{P} : \boldsymbol{\nabla}_0 \boldsymbol{\delta\varphi} d\Omega \; + \int_{\partial_{\mathrm{I}}\Omega_0} [\![\boldsymbol{\delta\varphi} \cdot \mathbf{P}]\!] \cdot \boldsymbol{N}^{-} d\partial\Omega = \int_{\partial_N \Omega_0} \overline{\boldsymbol{T}} \cdot \boldsymbol{\delta\varphi} d\partial\Omega$$

  - Introduction of a consistent numerical flux

$$\int_{\Omega_0} \mathbf{P} : \boldsymbol{\nabla}_0 \boldsymbol{\delta\varphi} d\Omega \; + \int_{\partial_{\mathrm{I}}\Omega_0} [\![\boldsymbol{\delta\varphi}]\!] \cdot \langle \mathbf{P} \rangle \cdot \boldsymbol{N}^{-} d\partial\Omega = \int_{\partial_N \Omega_0} \overline{\boldsymbol{T}} \cdot \boldsymbol{\delta\varphi} d\partial\Omega$$

- Discontinuous Galerkin (DG) methods (3)

$$\int_{\Omega_0} \mathbf{P} : \boldsymbol{\nabla}_0 \boldsymbol{\delta\varphi} d\Omega + \int_{\partial_I \Omega_0} [\![\boldsymbol{\delta\varphi} \cdot \mathbf{P}]\!] \cdot \boldsymbol{N}^- d\partial\Omega = \int_{\partial_N \Omega_0} \overline{\boldsymbol{T}} \cdot \boldsymbol{\delta\varphi} d\partial\Omega$$

  - Introduction of a consistent numerical flux

$$\int_{\Omega_0} \mathbf{P} : \boldsymbol{\nabla}_0 \boldsymbol{\delta\varphi} d\Omega + \int_{\partial_I \Omega_0} [\![\boldsymbol{\delta\varphi}]\!] \cdot \langle \mathbf{P} \rangle \cdot \boldsymbol{N}^- d\partial\Omega = \int_{\partial_N \Omega_0} \overline{\boldsymbol{T}} \cdot \boldsymbol{\delta\varphi} d\partial\Omega$$

  - Weak enforcement of the compatibility & symmetrization

$$\int_{\Omega_0} \mathbf{P} : \boldsymbol{\nabla}_0 \boldsymbol{\delta\varphi} d\Omega + \int_{\partial_I \Omega_0} [\![\boldsymbol{\delta\varphi}]\!] \cdot \langle \mathbf{P} \rangle \cdot \boldsymbol{N}^- d\partial\Omega + \int_{\partial_I \Omega_0} [\![\boldsymbol{\varphi}]\!] \cdot \langle \boldsymbol{C}^{\mathrm{el}} : \boldsymbol{\nabla}_{\mathbf{0}} \boldsymbol{\delta\varphi} \rangle \cdot \boldsymbol{N}^- d\partial\Omega$$

$$= \int_{\partial_N \Omega_0} \overline{\boldsymbol{T}} \cdot \boldsymbol{\delta\varphi} d\partial\Omega$$

- Discontinuous Galerkin (DG) methods (3)

$$\int_{\Omega_0} \mathbf{P} : \nabla_0 \boldsymbol{\delta\varphi} d\Omega + \int_{\partial_I \Omega_0} [\![\boldsymbol{\delta\varphi} \cdot \mathbf{P}]\!] \cdot \boldsymbol{N}^- d\partial\Omega = \int_{\partial_N \Omega_0} \overline{\boldsymbol{T}} \cdot \boldsymbol{\delta\varphi} d\partial\Omega$$

  - Introduction of a consistent numerical flux

$$\int_{\Omega_0} \mathbf{P} : \nabla_0 \boldsymbol{\delta\varphi} d\Omega + \int_{\partial_I \Omega_0} [\![\boldsymbol{\delta\varphi}]\!] \cdot \langle \mathbf{P} \rangle \cdot \boldsymbol{N}^- d\partial\Omega = \int_{\partial_N \Omega_0} \overline{\boldsymbol{T}} \cdot \boldsymbol{\delta\varphi} d\partial\Omega$$

  - Weak enforcement of the compatibility & symmetrization

$$\int_{\Omega_0} \mathbf{P} : \nabla_0 \boldsymbol{\delta\varphi} d\Omega + \int_{\partial_I \Omega_0} [\![\boldsymbol{\delta\varphi}]\!] \cdot \langle \mathbf{P} \rangle \cdot \boldsymbol{N}^- d\partial\Omega + \int_{\partial_I \Omega_0} [\![\boldsymbol{\varphi}]\!] \cdot \langle \boldsymbol{C}^{\mathrm{el}} : \nabla_0 \boldsymbol{\delta\varphi} \rangle \cdot \boldsymbol{N}^- d\partial\Omega$$

$$= \int_{\partial_N \Omega_0} \overline{\boldsymbol{T}} \cdot \boldsymbol{\delta\varphi} d\partial\Omega$$

  - Stabilization controlled by a parameter β_s for all mesh sizes h^s

$$\int_{\Omega_0} \mathbf{P} : \nabla_0 \boldsymbol{\delta\varphi} d\Omega + \int_{\partial_I \Omega_0} [\![\boldsymbol{\delta\varphi}]\!] \cdot \langle \mathbf{P} \rangle \cdot \boldsymbol{N}^- d\partial\Omega + \int_{\partial_I \Omega_0} [\![\boldsymbol{\varphi}]\!] \cdot \langle \boldsymbol{C}^{\mathrm{el}} : \nabla_0 \boldsymbol{\delta\varphi} \rangle \cdot \boldsymbol{N}^- d\partial\Omega$$

$$+ \int_{\partial_I \Omega_0} [\![\boldsymbol{\varphi}]\!] \otimes \boldsymbol{N}^- : \langle \frac{\beta_s \boldsymbol{C}^{\mathrm{el}}}{h^s} \rangle : [\![\boldsymbol{\delta\varphi}]\!] \otimes \boldsymbol{N}^- d\partial\Omega = \int_{\partial_N \Omega_0} \overline{\boldsymbol{T}} \cdot \boldsymbol{\delta\varphi} d\partial\Omega$$

[Noels & Radovitzky, IJNME 2006]

- Hybrid Discontinuous Galerkin/Extrinsic Cohesive Law method
  - Final DG formulation

$$\int_{\Omega_0} \mathbf{P} : \boldsymbol{\nabla}_0 \boldsymbol{\delta\varphi} d\Omega + \int_{\partial_I \Omega_0} [\![\boldsymbol{\delta\varphi}]\!] \cdot \langle \mathbf{P} \rangle \cdot \boldsymbol{N}^- d\partial\Omega + \int_{\partial_I \Omega_0} [\![\boldsymbol{\varphi}]\!] \cdot \langle \boldsymbol{C}^{\text{el}} : \boldsymbol{\nabla_0 \delta\varphi} \rangle \cdot \boldsymbol{N}^- d\partial\Omega$$
$$+ \int_{\partial_I \Omega_0} [\![\boldsymbol{\varphi}]\!] \otimes \boldsymbol{N}^- : \langle \frac{\beta_s \boldsymbol{C}^{\text{el}}}{h^s} \rangle : [\![\boldsymbol{\delta\varphi}]\!] \otimes \boldsymbol{N}^- d\partial\Omega = \int_{\partial_N \Omega_0} \overline{\boldsymbol{T}} \cdot \boldsymbol{\delta\varphi} d\partial\Omega$$

    - Interface terms integrated on an interface element

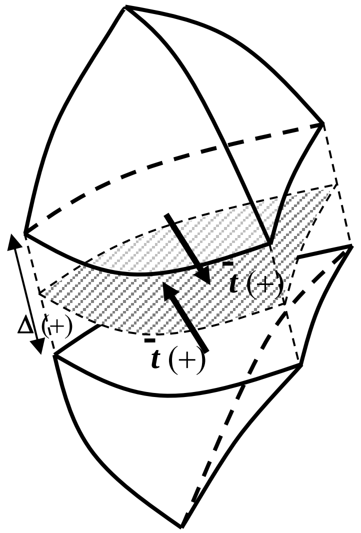

Université de Liège

- Hybrid Discontinuous Galerkin/Extrinsic Cohesive Law method
  - Final DG formulation

$$\int_{\Omega_0} \mathbf{P} : \nabla_0 \boldsymbol{\delta\varphi} d\Omega + \int_{\partial_I \Omega_0} [\![\boldsymbol{\delta\varphi}]\!] \cdot \langle \mathbf{P} \rangle \cdot \boldsymbol{N}^- d\partial\Omega + \int_{\partial_I \Omega_0} [\![\boldsymbol{\varphi}]\!] \cdot \langle \boldsymbol{C}^{\mathrm{el}} : \nabla_0 \boldsymbol{\delta\varphi} \rangle \cdot \boldsymbol{N}^- d\partial\Omega$$
$$+ \int_{\partial_I \Omega_0} [\![\boldsymbol{\varphi}]\!] \otimes \boldsymbol{N}^- : \langle \frac{\beta_s \boldsymbol{C}^{\mathrm{el}}}{h^s} \rangle : [\![\boldsymbol{\delta\varphi}]\!] \otimes \boldsymbol{N}^- d\partial\Omega = \int_{\partial_N \Omega_0} \overline{\boldsymbol{T}} \cdot \boldsymbol{\delta\varphi} d\partial\Omega$$

    - Interface terms integrated on an interface element
  - Taking advantage of the interface elements
    - Check is fracture criterion is reached (α: 0->1)
    - If so, use the extrinsic cohesive law

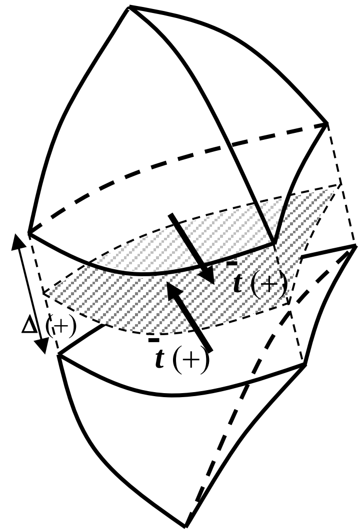

$$\int_{\Omega_0} \mathbf{P} : \nabla_0 \boldsymbol{\delta\varphi} d\Omega + \alpha \int_{\partial_I \Omega} [\![\boldsymbol{\delta\varphi}]\!] \cdot \bar{\boldsymbol{t}} \cdot \boldsymbol{n}^- d\partial\Omega +$$

$$(1-\alpha) \int_{\partial_I \Omega_0} [\![\boldsymbol{\delta\varphi}]\!] \cdot \langle \mathbf{P} \rangle \cdot \boldsymbol{N}^- d\partial\Omega +$$
$$(1-\alpha) \int_{\partial_I \Omega_0} [\![\boldsymbol{\varphi}]\!] \cdot \langle \boldsymbol{C}^{\mathrm{el}} : \nabla_0 \boldsymbol{\delta\varphi} \rangle \cdot \boldsymbol{N}^- d\partial\Omega +$$
$$(1-\alpha) \int_{\partial_I \Omega_0} [\![\boldsymbol{\varphi}]\!] \otimes \boldsymbol{N}^- : \langle \frac{\beta_s \boldsymbol{C}^{\mathrm{el}}}{h^s} \rangle : [\![\boldsymbol{\delta\varphi}]\!] \otimes \boldsymbol{N}^- d\partial\Omega =$$
$$\int_{\partial_N \Omega_0} \overline{\boldsymbol{T}} \cdot \boldsymbol{\delta\varphi} d\partial\Omega$$

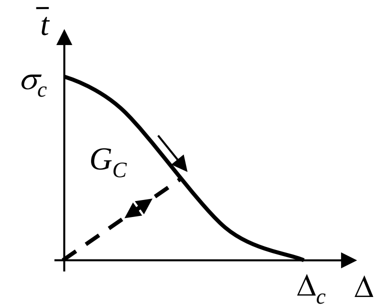

- Efficient // implementation
  - Based on the ghost-faces method
  - Initial mesh

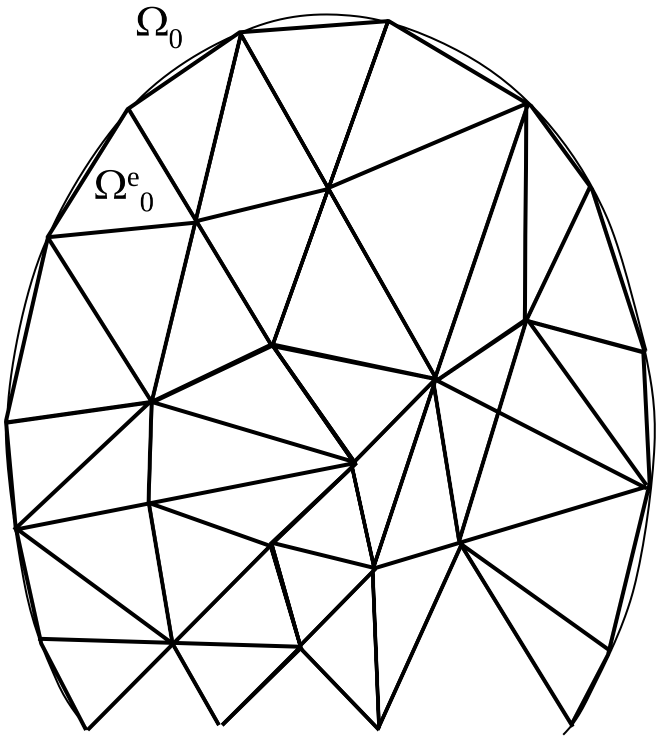

- Efficient // implementation (2)
  - Based on the ghost-faces method
  - Partitioned mesh (METIS)
    - Internal forces can be computed
      - At bulk elements
      - At interface elements in the partitions

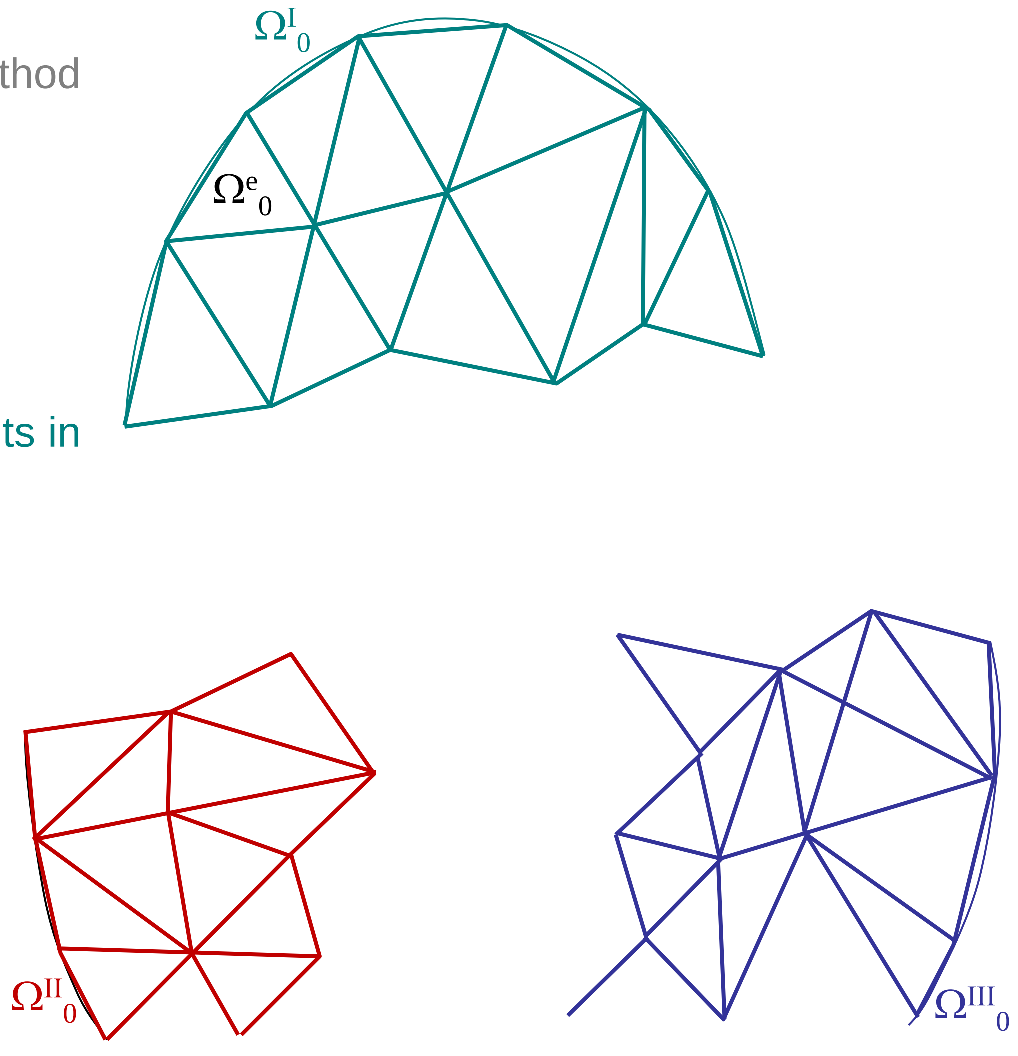

- Efficient // implementation (2)
  - Based on the ghost-faces method
  - Partitioned mesh (METIS)
    - Internal forces can be computed
      - At bulk elements
      - At interface elements in the partitions
    - Interface elements at processors boundaries?

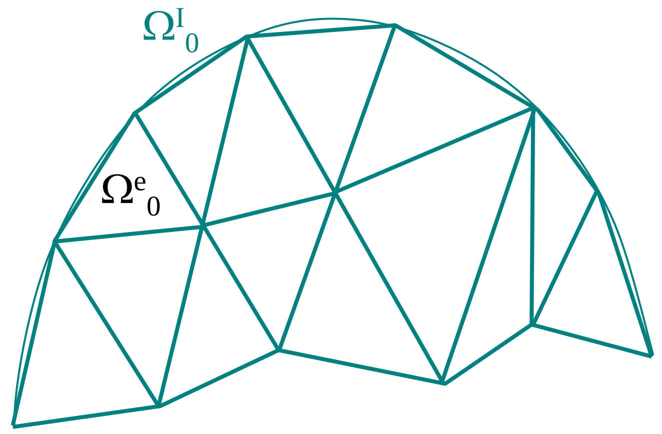

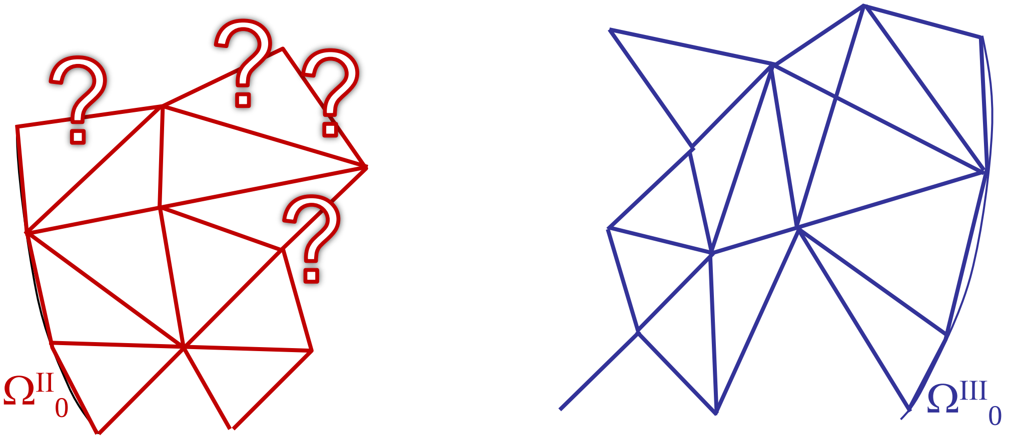

- Efficient // implementation (3)
  - Based on the ghost-faces method

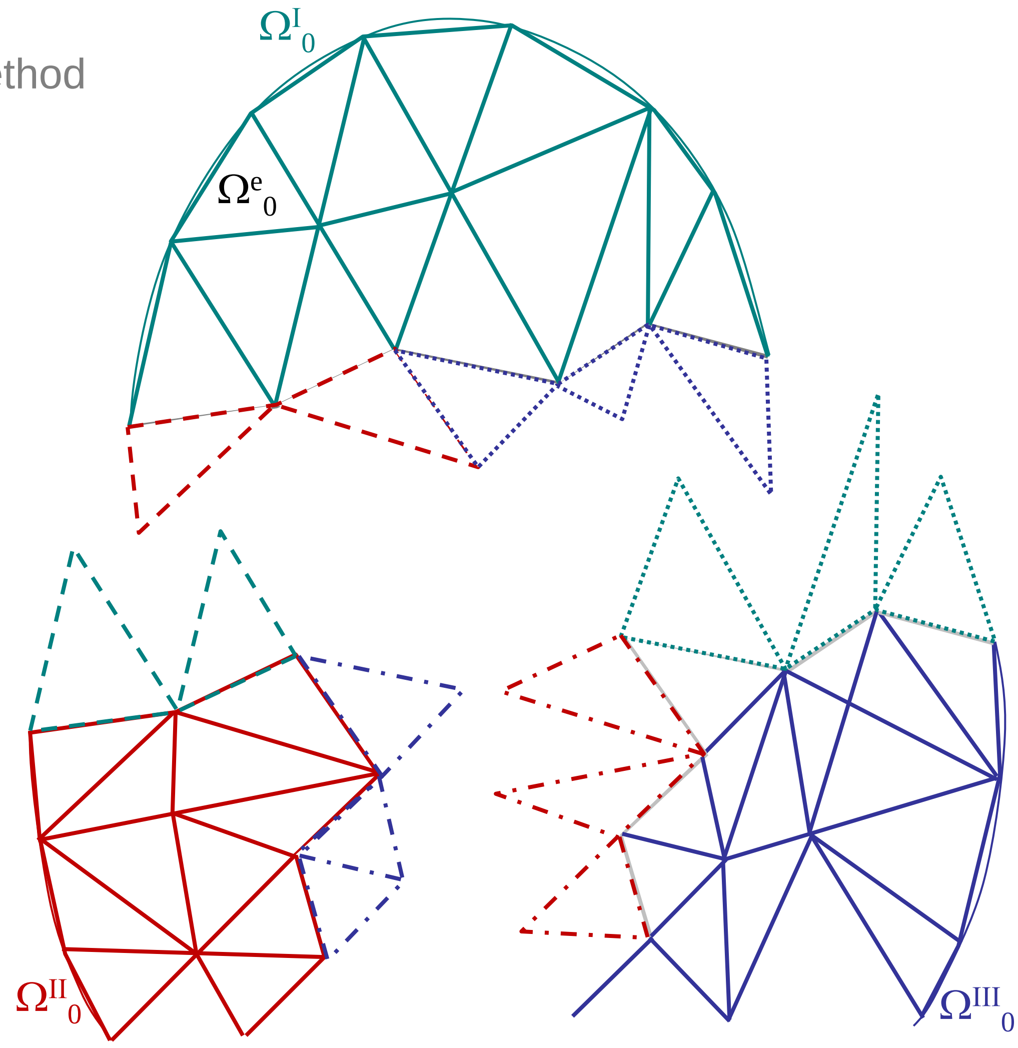

  - Create ghost elements
    - Internal forces can be computed at processors boundaries interfaces
    - If deformation of ghost elements is correct

- Efficient // implementation (4)
  - Based on the ghost-faces method

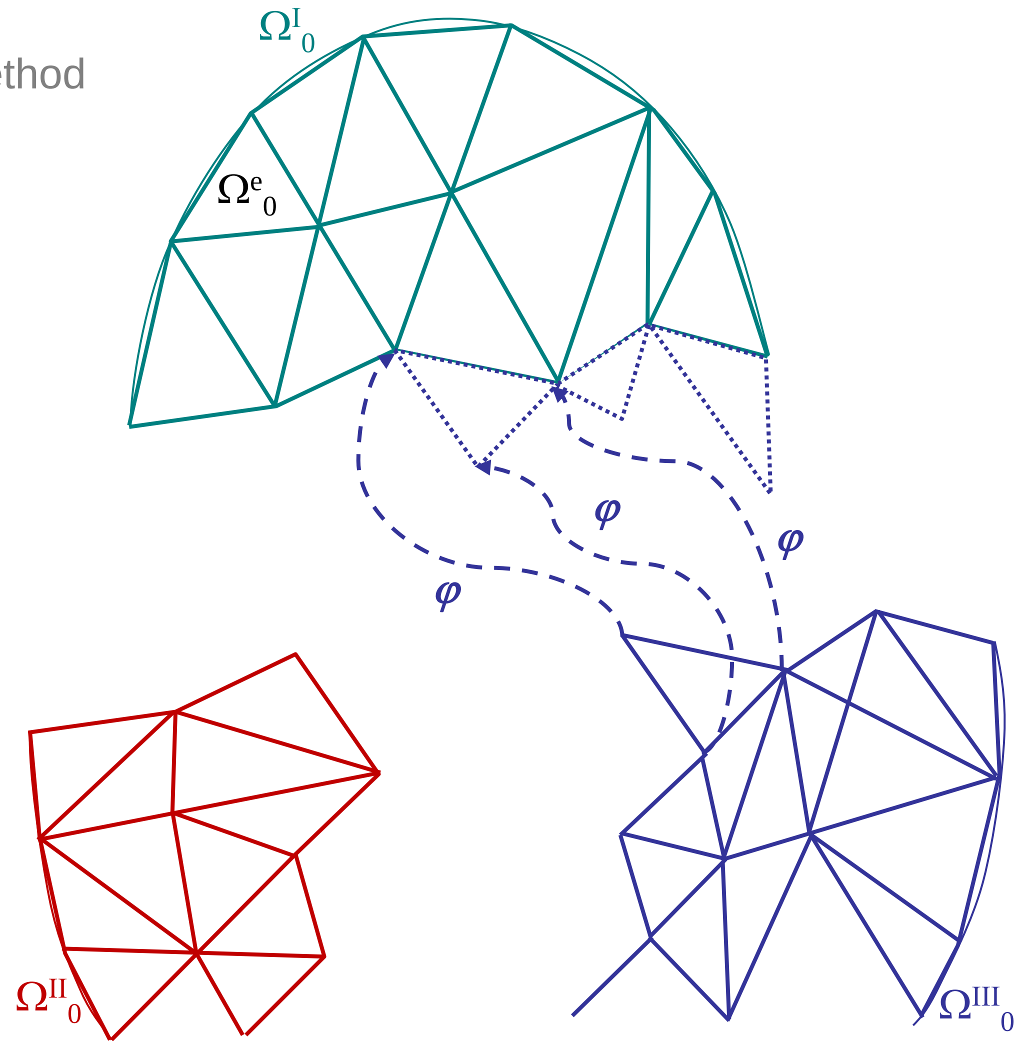

  - Update positions of ghost elements nodes
    - Only exchange

Application to intra-laminar failure of composites

- Composite materials
  - UD carbon-fiber (60%) reinforced epoxy
    - Elasto-plastic matrix
    - Transverse anisotropic fibers
    - Interface failure:
      - σ_C = 45 MPa, G_C = 100 J/m^2
    - Intra-matrix failure:
      - σ_C = 83 MPa, G_C = 78 J/m^2 [Sato et al., 1986]

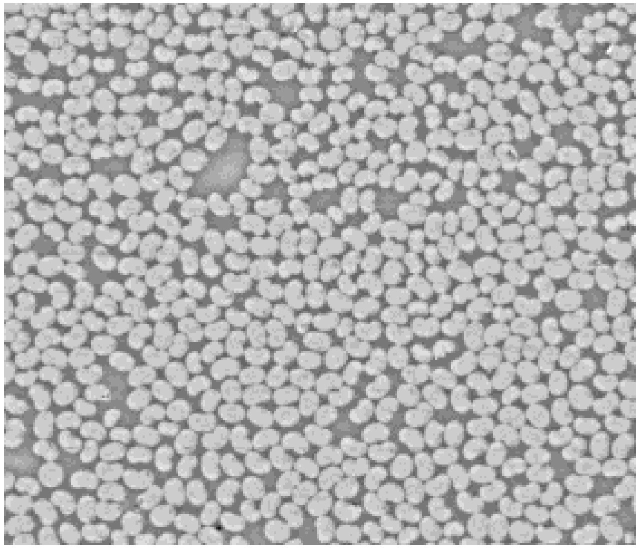

  - Transverse loading experiments

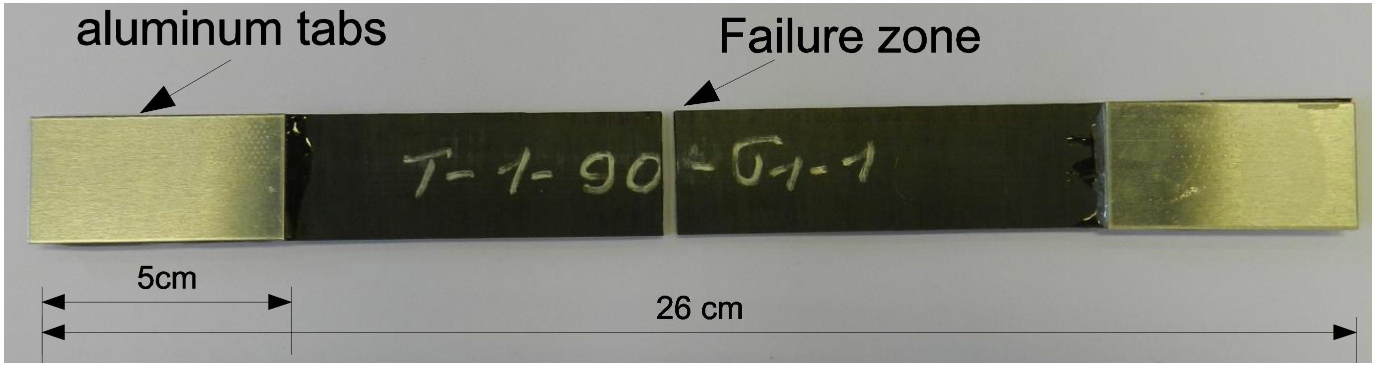

- Micro-models
  - Study of the cell size effect (3D random cells)

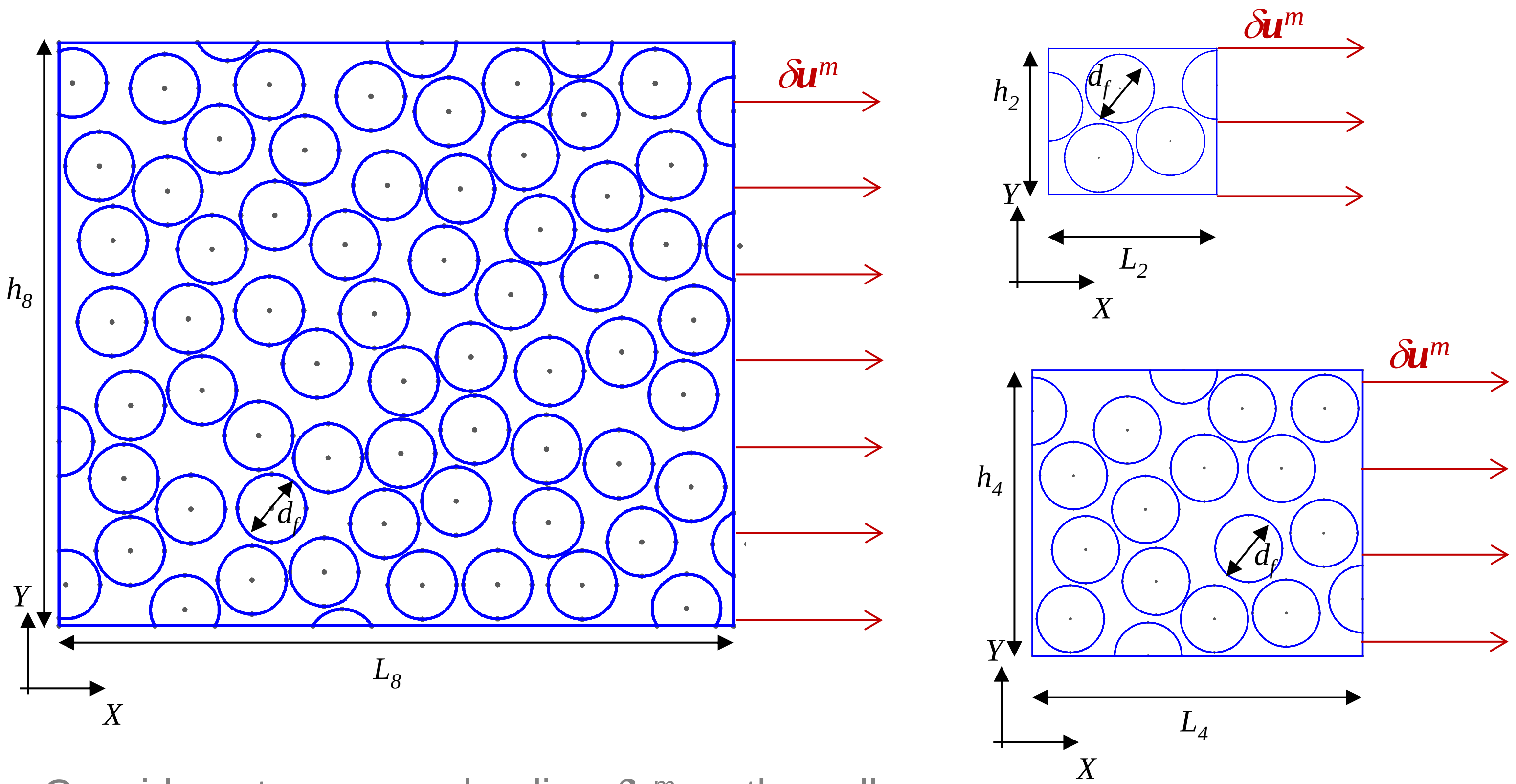

  - Consider a transverse loading $\delta\mathbf{u}^m$ on the cells

- Simulations

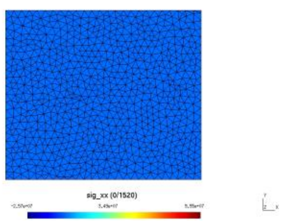

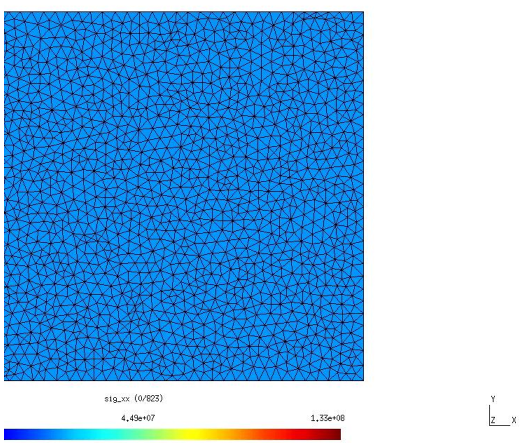

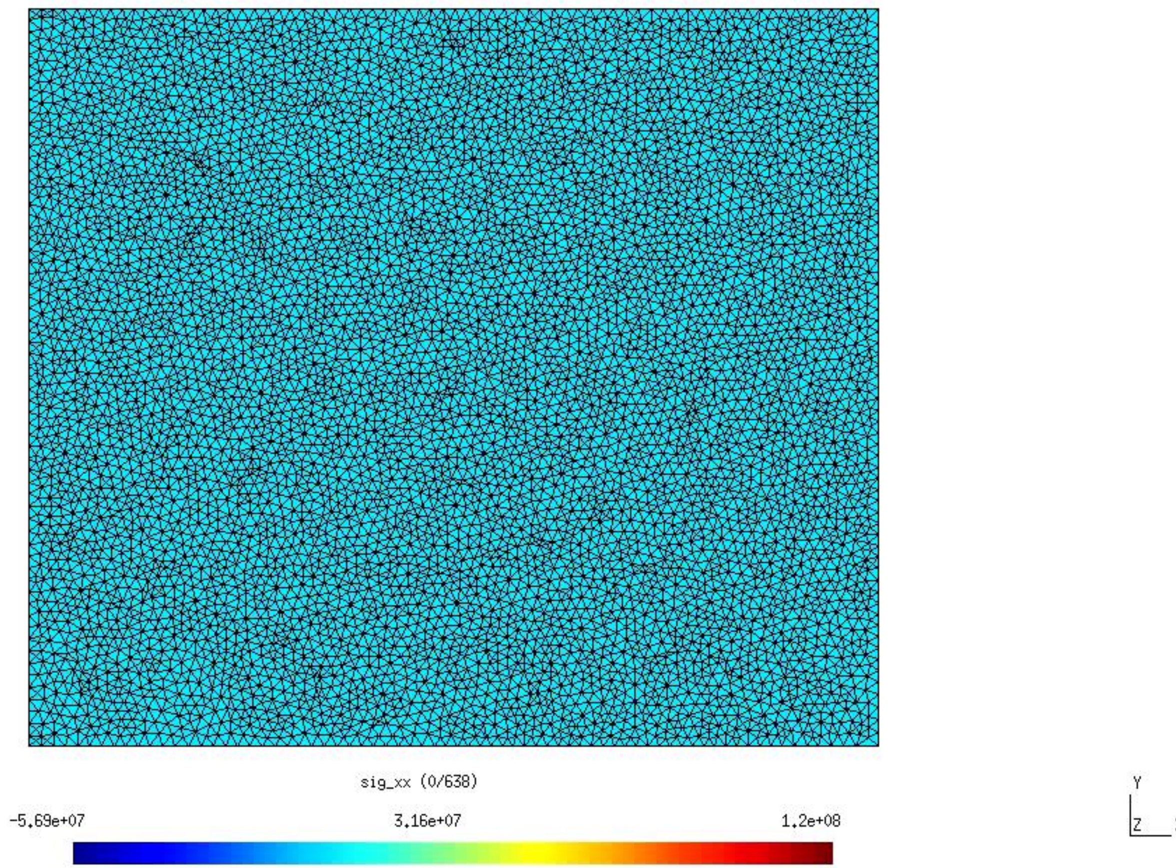

Application to intra-laminar failure of composites

- Micro-Meso fracture model for intra-laminar failure
  - Epoxy-CF (60%), transverse loading
  - 3 stages captured
  - Cell size effect

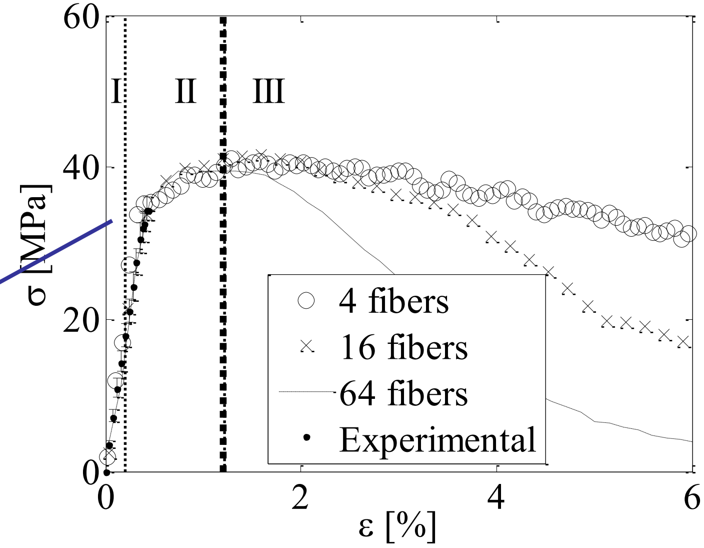

Elastic response

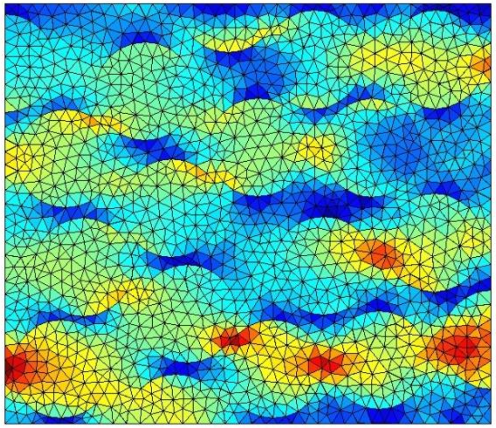

Application to intra-laminar failure of composites

- Micro-Meso fracture model for intra-laminar failure
  - Epoxy-CF (60%), transverse loading
  - 3 stages captured
  - Cell size effect

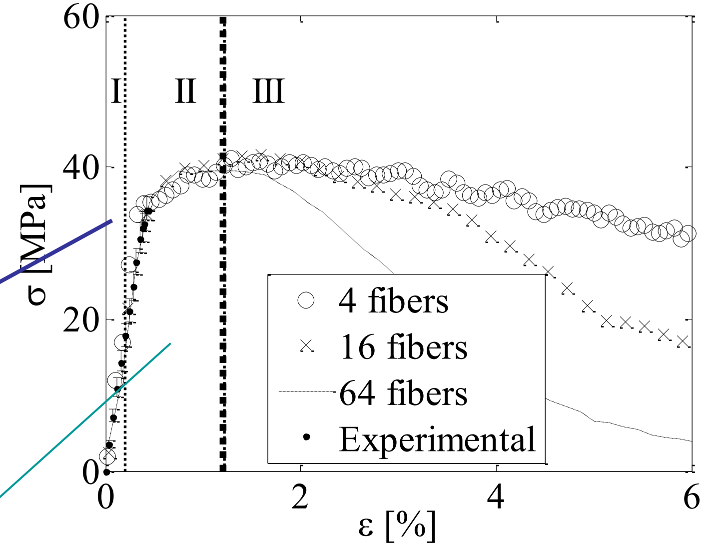

Elastic response

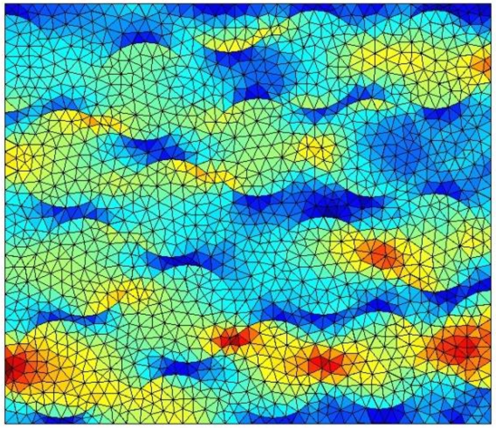

Damage due to debonding

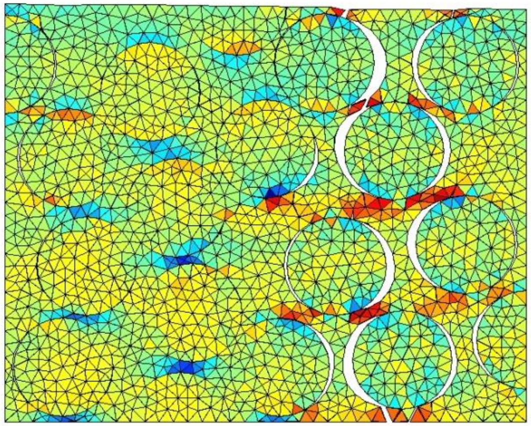

Application to intra-laminar failure of composites

- Micro-Meso fracture model for intra-laminar failure
  - Epoxy-CF (60%), transverse loading
  - 3 stages captured
  - Cell size effect

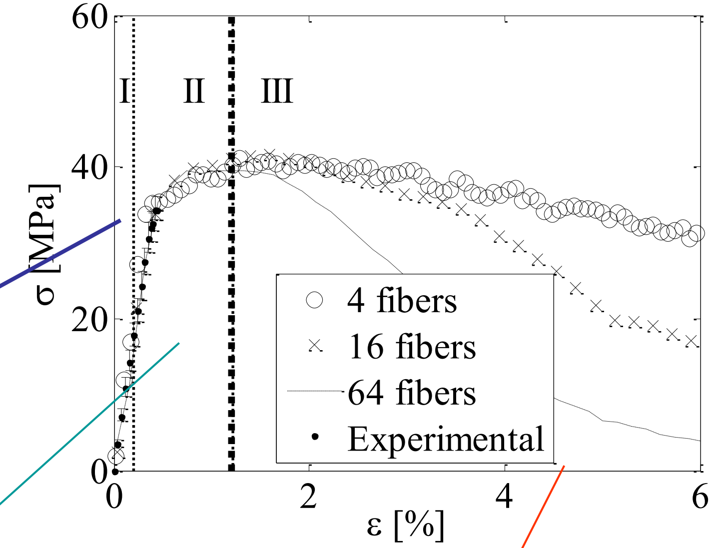

Elastic response

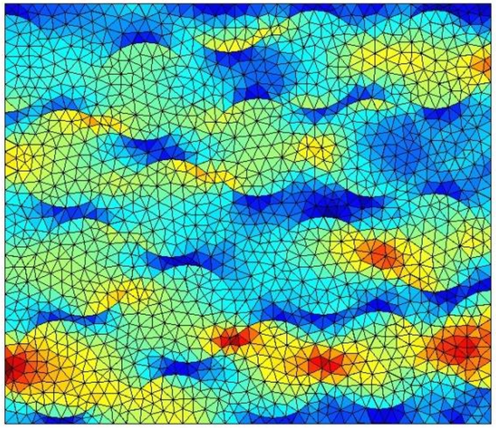

Damage due to debonding

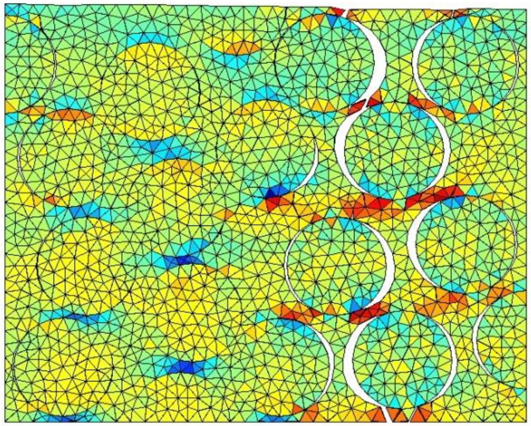

Meso-crack

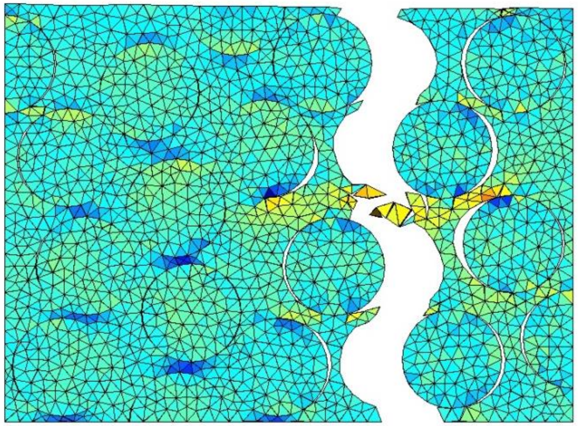

- Micro-Meso fracture model for intra-laminar failure (2)
  - Scale transition after softening onset
    - Should not depend on the RVE size

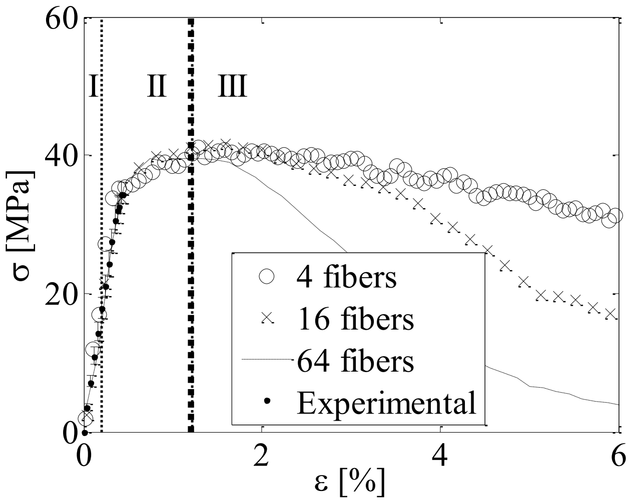

Application to intra-laminar failure of composites

- Micro-Meso fracture model for intra-laminar failure (2)
  - Scale transition after softening onset
    - Should not depend on the RVE size
  - The displacement $\delta\boldsymbol{u}^m$ of the RVE needs to be corrected
    - Mesoscopic surface traction directly obtained

$$\boldsymbol{\delta\bar{t}} = \boldsymbol{\sigma} \cdot \boldsymbol{e}_X$$

    - Compute a mesoscopic opening (increment)

$$\delta\boldsymbol{u}^M = \delta\boldsymbol{u}^m - L_{\text{cell}}\boldsymbol{C}^{\text{el}^{-1}} : \boldsymbol{e}_X \otimes \boldsymbol{e}_X \cdot \boldsymbol{\delta\bar{t}} - \delta\boldsymbol{u}_0^m$$

which accounts for the change in the structural stiffness $\boldsymbol{C}$ due to irreversible processes

$$\delta\boldsymbol{u}_0^m = L_{\text{cell}}\left(\boldsymbol{C}^{-1} - \boldsymbol{C}^{\text{el}^{-1}}\right) : \boldsymbol{e}_X \otimes \boldsymbol{e}_X \cdot \boldsymbol{\delta\bar{t}}$$

[Verhoosel et al., IJNME 2010]

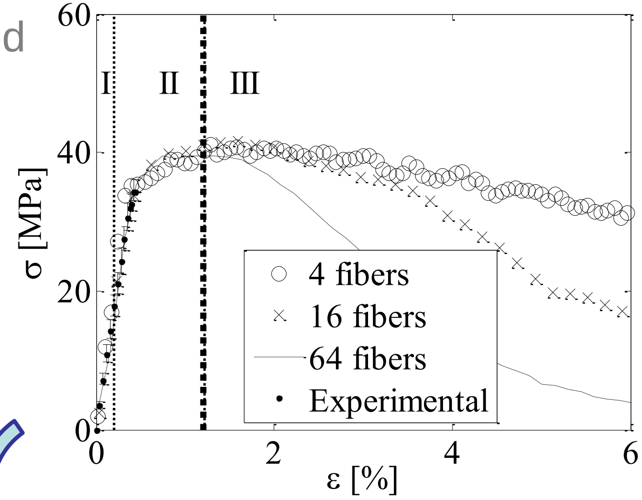

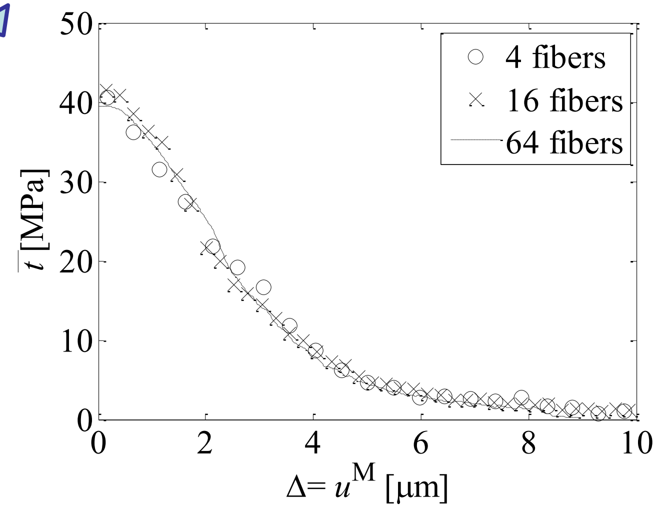

- Micro-Meso fracture model for intra-laminar failure (2)
  - Scale transition after softening onset
    - Should not depend on the RVE size
  - The displacement $\delta \boldsymbol{u}^m$ of the RVE needs to be corrected
    - Mesoscopic surface traction directly obtained

$$\boldsymbol{\delta \bar{t}} = \boldsymbol{\sigma} \cdot \boldsymbol{e}_X$$

    - Compute a mesoscopic opening (increment)

$$\delta \boldsymbol{u}^M = \delta \boldsymbol{u}^m - L_{\text{cell}} {\boldsymbol{C}^{\text{el}}}^{-\mathbf{1}} : \boldsymbol{e}_X \otimes \boldsymbol{e}_X \cdot \boldsymbol{\delta \bar{t}} - \delta \boldsymbol{u}_0^m$$

which accounts for the change in the structural stiffness $\boldsymbol{C}$ due to irreversible processes

$$\delta \boldsymbol{u}_0^m = L_{\text{cell}} \left(\boldsymbol{C}^{-\mathbf{1}} - {\boldsymbol{C}^{\text{el}}}^{-\mathbf{1}} \right) : \boldsymbol{e}_X \otimes \boldsymbol{e}_X \cdot \boldsymbol{\delta \bar{t}}$$

[Verhoosel et al., IJNME 2010]

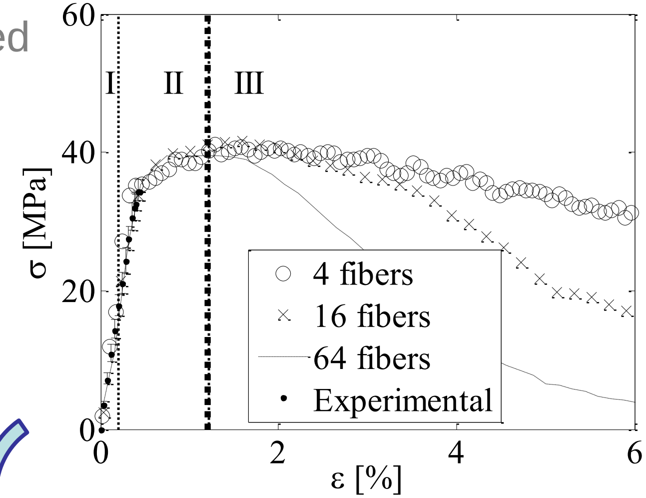

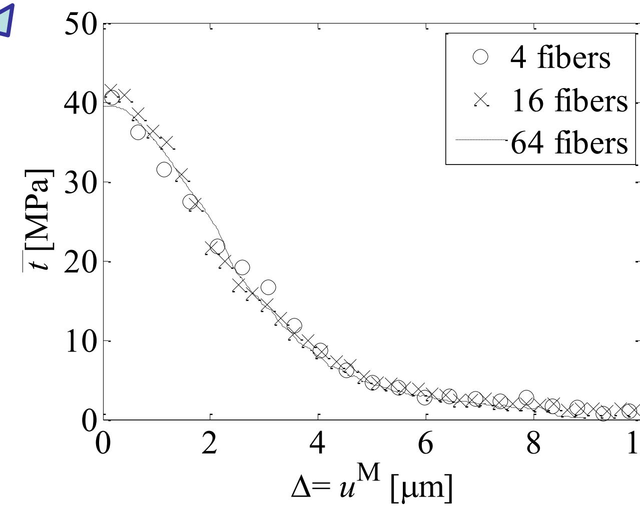

  - Corresponds to a meso-scale cohesive law
    - Area converges to the apparent energy release rate of the composite: 122 J/m2
    - To be compared to G_C of epoxy (78 J/m2)

Application to intra-laminar failure of composites

- Comparison with experiments
  - Loading curve can be compared up to strain softening
  - Similar failure mode

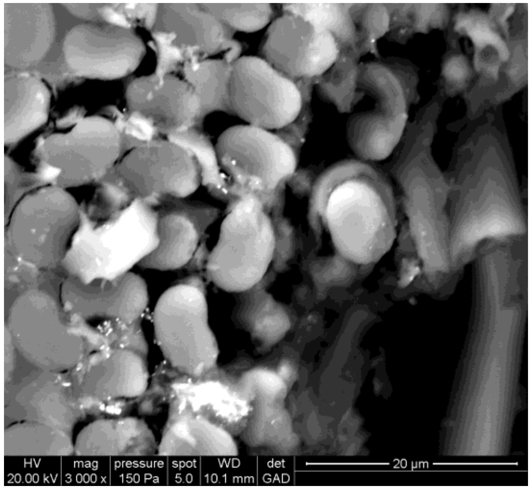

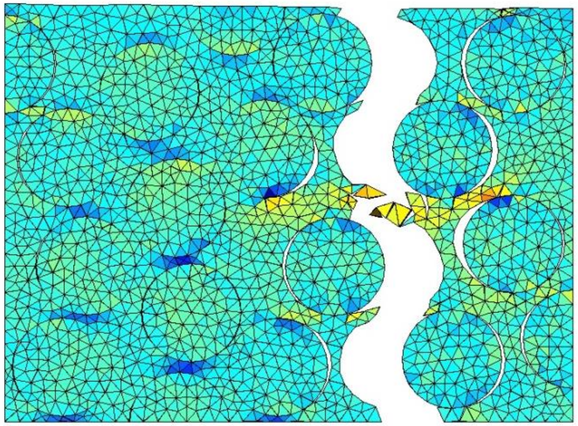

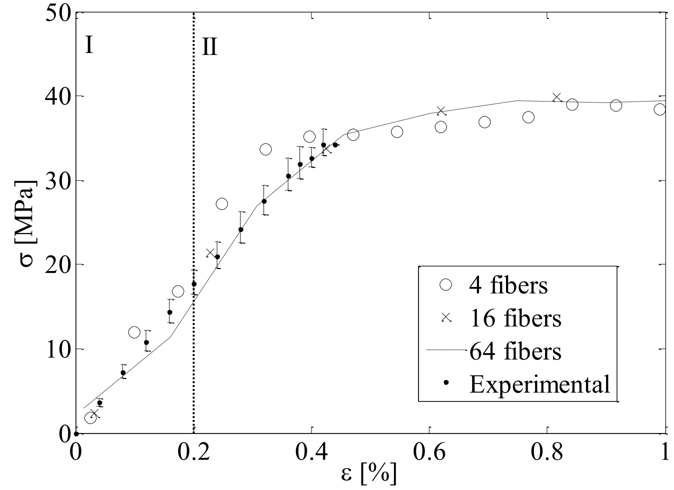

Conclusions

- Hybrid DG/ECL method
  - Efficient parallel computational method
  - Can be used to simulate micro failure
- Micro-meso model
  - Meso-scale cohesive law can be extracted from simulations
  - Small cells can provide accurate results
- Perspectives
  - Loading direction effects
  - Computational multiscale failure